

Measuring multimegavolt pulsed voltages using Compton-generated electrons

S. B. Swanekamp^{a),b)}, B. V. Weber, N. R. Pereira,^{c)} D. D. Hinshelwood, S. J. Stephanakis,^{b)} and F. C. Young^{b)}

Plasma Physics Division, Naval Research Laboratory, Washington, DC 20375

(Received 26 February 2003; accepted 25 September 2003)

The “Compton–Hall” voltmeter is a radiation-based voltage diagnostic that has been developed to measure voltages on high-power (TW) pulsed generators. The instrument collimates photons generated from bremsstrahlung produced in the diode onto an aluminum target to generate Compton-generated electrons. Permanent magnets bend the Compton electron orbits that escape the target toward a silicon *pin* diode detector. A GaAs photoconductive detector (PCD) detects photons that pass through the Compton target. The diode voltage is determined from the ratio of the electron dose in the *pin* detector to the x-ray dose in the PCD. The Integrated Tiger Series of electron–photon transport codes is used to determine the relationship between the measured dose ratio and the diode voltage. Variations in the electron beam’s angle of incidence on the bremsstrahlung target produce changes in the shape of the photon spectrum that lead to large variations in the voltage inferred from the voltmeter. The voltage uncertainty is minimized when the voltmeter is fielded at an angle of 45° with respect to the bremsstrahlung target. In this position, the photon spectra for different angles of incidence all converge onto a single spectrum reducing the uncertainty in the voltage to less than 10% for voltages below 4 MV. Higher and lower voltages than the range considered in this article can be measured by adjusting the strength of the applied magnetic field or the position of the electron detector relative to the Compton target. The instrument was fielded on the Gamble II pulsed-power generator configured with a plasma opening switch. Measurements produced a time-dependent voltage with a peak (3.7 MV) that agrees with nuclear activation measurements and a pulse shape that is consistent with the measured radiation pulse shape. © 2004 American Institute of Physics. [DOI: 10.1063/1.1628843]

I. INTRODUCTION

The presence of high-energy charged particles and plasmas makes measuring the voltage in high-power (TW) diodes difficult. In many applications of these diodes, a good voltage measurement is crucial for interpreting the experimental results. Many different techniques have been tried to measure the voltage with varying degrees of success. Conventional electrical techniques, such as capacitive monitors, work well in a liquid-dielectric-filled pulse-forming line but they usually require a substantial inductive correction to obtain the voltage at the diode. The presence of plasmas and/or vacuum electron flow generally introduce large uncertainties in the inferred diode voltage. Inferring the diode voltage from the radiation produced is attractive for situations where the electron beam energy in the diode corresponds to the voltage since the photons generated in the diode readily escape the surrounding vacuum vessel and are easily detected. Differential filtering techniques determine the voltage from the ratios of dose rates measured in Si *pin* diodes [or from dose ratios measured with thermoluminescent dosimeters (TLDs)] with carefully chosen filter materials and thicknesses.^{1,2} This method works well for voltages between

0.5 and 2 MV, where photoelectric absorption dominates the filter attenuation, but is difficult for higher voltages because the photon attenuation length becomes insensitive to changes in the voltage. Other methods that rely on well-known energy thresholds for nuclear reactions, such as the photoexcitation of nuclear isomers^{3,4} or photoneutron generation,⁵ are also suitable but they are only capable of determining the peak diode voltage.

In the instrument described in this article, bremsstrahlung from the diode is filtered and collimated onto an aluminum target producing a shower of Compton electrons. Permanent magnets bend the Compton electron orbits toward a Si *pin* diode where a fraction of them are detected. A GaAs photoconductive detector (PCD) is used to measure the x-ray dose from photons that pass through both the filter and the Compton target. The diode voltage is determined from the ratio of the electron dose measured by the Si *pin* diode to the x-ray dose measured by the PCD. A PCD was used as the photon detector and a *pin* diode was used as the electron detector because the electron dose is expected to be a few percent of the photon dose. This requires that the electron detector be much more sensitive than the photon detector. Therefore, a *pin* diode was chosen with a relatively large area and a large depletion depth. A PCD was chosen for the photon detector since it is less sensitive than the *pin* diode.

This device is called the Compton–Hall (CH) voltmeter

^{a)}Electronic mail: swane@calvin.nrl.navy.mil

^{b)}Also at Titan/Jaycor, McLean, VA 22102.

^{c)}Also at Ecopulse, Inc., P.O. Box 528, Springfield, VA 22150.

in a loose analogy to the Hall effect in conductors. Here, photons play the role of the driving electric field to generate a current of Compton electrons. To continue the analogy further, a current is generated perpendicular to the magnetic field that is similar to the Hall current, which in our case is a current of free electrons that is measured by its dose rate. This device is also similar to Compton spectrometers, some of which have been used to measure the bremsstrahlung spectrum from pulsed-power diodes.^{6,7} The CH voltmeter differs from these spectrometers in that it does not determine the entire spectrum from an array of electron detectors but relies on the sensitivity of the end-point energy to the ratio of the dose in a single electron detector to the photon dose. It is also relatively small and inexpensive compared to traditional spectrometers, and the interpretation of the data is straightforward, making it feasible for end-point voltage measurements in a wide variety of pulsed-power diodes.

Like all radiation-based voltage diagnostics, the CH voltmeter implicitly assumes that changes in the diode voltage are slow compared to the electron transit time across the diode gap. In this case, there is a direct correlation between the electrostatic voltage across the diode and the electron energy incident on the bremsstrahlung target. The principle of the CH voltmeter was demonstrated previously for beam voltages between 1 and 2 MV using a low-power Van de Graaff generator and time-integrated TLDs.⁸ In this article, the analysis of the voltmeter is extended to 6 MV and a time-dependent voltage measurement with a peak voltage of 3.7 MV is demonstrated. The sensitivity of the voltmeter to the electron angle of incidence on the bremsstrahlung target is also evaluated and a method to minimize this sensitivity is presented.

II. COMPUTATIONS AND ANALYSIS

The geometry of the CH voltmeter is shown in Fig. 1. The collimator consists of a 10 cm tungsten cube with a 1-cm-diam hole bored through the center of one of the faces. A 0.635-cm-thick tungsten filter at the entrance of the collimator transmits harder parts of the bremsstrahlung spectrum and keeps the detectors from saturating. A 0.2-cm-thick aluminum Compton target is located at the end of the collimator. The Compton target is thick enough to stop any Compton electrons generated in the collimator. A 10 cm×10 cm×5 cm brass section, immediately behind the Compton target, has a 1.6 cm×2.5 cm×3.5 cm open interior that forms the Compton chamber. The Compton chamber is at atmospheric pressure. A 1-cm-diam hole, located at the end of the Compton chamber, leads to the PCD detector, which is embedded in a 10 cm aluminum cube. The PCD consists of a 6-mm-diam ×1-mm-thick GaAs disk packaged in a brass cylinder with a 0.5-mm-thick aluminum front cover. Permanent magnets provide either a 4.4 or 6.0 kG magnetic field that bends the electron orbits toward the Si *pin* diode and prevents them from reaching the PCD. The 0.564-cm-diam Si *pin* diode is operated at a bias of -600 V to provide a depletion layer of 500 μm. The *pin* diode is mounted in a 1.6 cm×3.75 cm ×2.5 cm aluminum holder that slides into a slot in the brass section. When installed in the voltmeter, the *pin* diode is

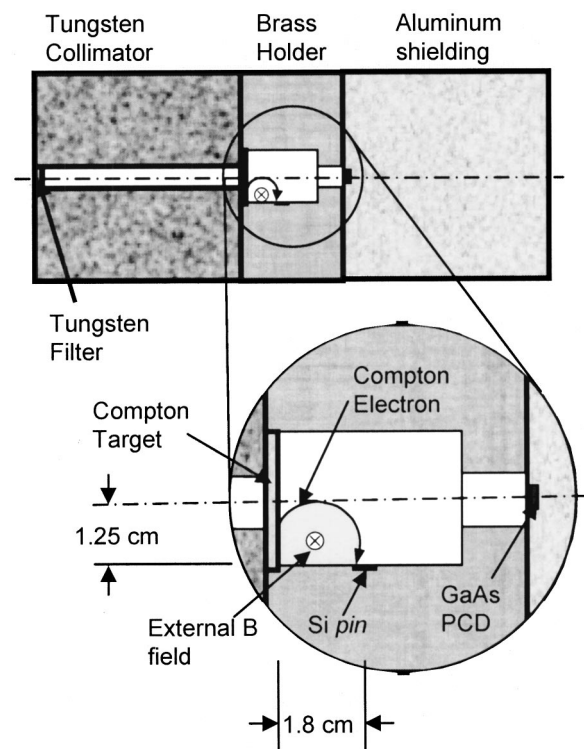


FIG. 1. Schematic of the Compton-Hall voltmeter geometry. The smallest Larmor radius and some critical dimensions are shown in the blowup.

located 1.25 cm off the center line of the device and mounted flush with the surface of the Compton chamber. The *pin* diodes could be fielded at either 1.8 cm (position 1) or 2.8 cm (position 2) downstream of the Compton target.

A qualitative understanding of the voltmeter can be obtained from the Larmor radius of a Compton electron, which is given by

$$r_L = \frac{mc^2 \sqrt{\gamma^2 - 1}}{eB}, \quad (1)$$

where m is the electron rest mass, c is the speed of light, γ is the relativistic factor, e is the magnitude of the electron charge, and B is the magnetic field strength. (We will use cgs units throughout this article unless otherwise stated.) Equation (1) shows that the magnetic field strength and the location of the *pin* diode with respect to the Compton target determine the energy range of electrons that reach the *pin* diode. Therefore, the sensitive voltage range of the instrument can be adjusted by changing either the magnetic field strength or the location of the *pin* diode relative to the Compton target.

In general, the angular distribution and energy spectrum of electrons emerging from the Compton target is very complex, making a detailed analysis of the voltmeter using Eq. (1) difficult. Sample electron orbits are given in Ref. 8. However, an important limiting orbit is the smallest radius circle between the Compton target and the *pin* diode. This orbit corresponds to the lowest energy electrons that reach the *pin* diode, and hence, gives an approximate indication of the lowest diode voltage that can be measured. The smallest r_L is approximately $\frac{1}{2}$ the shortest distance between the Compton

target and the *pin* diode, as shown in Fig. 1. With the *pin* diode located 1.8 cm (2.8 cm) from the Compton target the smallest Larmor radius is 0.8 cm (1.3 cm). Therefore, with $B=4.4$ kG and the detector in position 1 (position 2) only electrons with energies above 0.7 MeV (1.3 MeV) reach the detector. The electron range in silicon at these energies exceeds the 500 μm depletion depth so only a portion of the electron energy is absorbed in the *pin* diode.

Detailed analysis of the voltmeter is performed using the Integrated Tiger Series (ITS) of electron-photon transport codes.⁹ The relevant photon interactions followed by the ITS include Compton scattering, photoelectric absorption, and pair production. The relevant electron interactions followed by the ITS code include collisional energy loss to ionization and excitation, radiation loss to and production of bremsstrahlung, and *K*- and *L*-shell ionization events that produce characteristic x-ray fluorescence lines and Auger electrons. A more-detailed description of the physics treated in the ITS code and the numerical methods used is available in Ref. 10. The voltmeter analysis is split into three separate calculations: (1) a detailed three-dimensional (3D) calculation of the spectral response of the detectors to monoenergetic photons incident on the Compton target, (2) a one-dimensional (1D) calculation of the conversion of an incident electron spectrum on the bremsstrahlung target into an equivalent photon point source, and (3) conversion of the photon spectrum from step (2) into the dose in each detector by convolving it with the spectral response calculated in step (1) and any filters. The advantage of separating the calculations in this manner is that the electron distribution on the bremsstrahlung target can be changed easily without having to redo lengthy 3D simulations of the CH voltmeter geometry. By separating the calculations in this manner, the Compton-generated electrons that exist between the bremsstrahlung target and the voltmeter are neglected. This is not a serious issue since the current of Compton electrons that reach the voltmeter is many orders of magnitude smaller than the primary electron beam so that any radiation produced by these electrons is negligible. The absorbed dose for a general photon spectrum can then be calculated from

$$\frac{\text{Dose}}{Q_e} = \int \rho_{\text{Det}}(h\nu) F(h\nu, \theta) \frac{d\Phi_S}{d(h\nu)} d(h\nu), \quad (2)$$

where Q_e is the incident electron charge on the bremsstrahlung target, $\rho_{\text{Det}}(h\nu)$ is the spectral response [dose per photon flux] for either the PCD or the Si *pin* diode, $F(h\nu, \theta)$ is the attenuation from the vacuum vessel and any other filters between the source and the detector, θ is the viewing angle, and $d\Phi_S/d(h\nu)$ is the differential photon flux spectrum per incident electron charge from the bremsstrahlung source.

The calculated spectral responses of the voltmeter detectors for $B=4.4$ kG are shown in Fig. 2. In this calculation, 20 million primary photons are used, which results in a statistical uncertainty of less than 5%. It is important to note that Compton scattering and fluorescence in the collimator were treated in the code by applying the incident photon flux across the face of the tungsten collimator. In addition, scattering and fluorescence in the brass holder as well as other parts of the voltmeter were also self-consistently included in

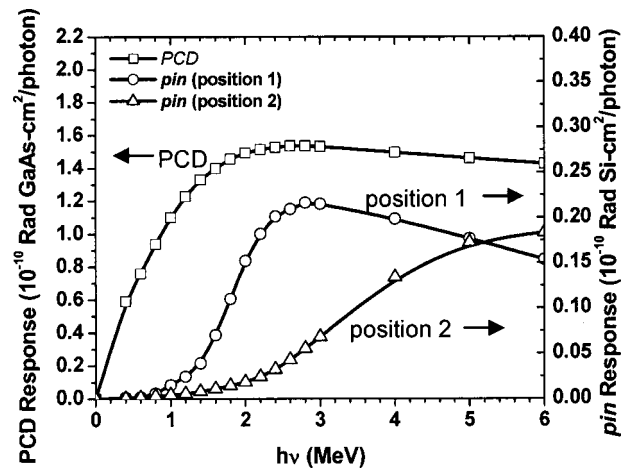


FIG. 2. Calculated spectral responses of the PCD and *pin* diode used in the Compton-Hall voltmeter for $B=4.4$ kG. The *pin* diode is located either 1.8 cm (position 1) or 2.8 cm (position 2) from the Compton target.

the calculations. However, no attempt was made to model room scattering, which could be present in any real application of the voltmeter. Instead, efforts were made in the experiments described below to minimize room scatter by surrounding the voltmeter with an appropriate amount of lead. The residual signals from room scattering were measured by blocking the entrance of the CH voltmeter with 10 cm of tungsten. The PCD signal was about 1% and the *pin* signal was about 20% of the signals without the tungsten. This background signal is subtracted before obtaining dose ratios. It is important to note that the spectral responses of the *pin* diode are from Compton-generated electrons, whose orbits are bent towards the detectors by an applied magnetic field. With the *pin* diode located in position 1 (position 2) there is little dose in the *pin* diode for photon energies less than 0.7 MeV (1.3 MeV). This is consistent with the minimum energy obtained above from the Larmor radius. The PCD response is nearly constant for photon energies above 2 MeV because the 0.5-mm-thick aluminum front cover is too thin to prevent Compton electrons generated inside the GaAs from escaping. The *pin* diode response at position 1 peaks and begins to decrease for photon energies above 3 MeV. In this case, the decrease is caused by the escape of knock-on electrons from the detector generated by electrons incident from the Compton target. This is not a major problem for voltages in the 2–5 MV range since the majority of the photons produced are well below 3 MeV. For higher voltages it would be beneficial to optimize the detector responses for the expected photon energies by choosing appropriate thickness front covers.

In general, the photon spectrum reaching the Compton target depends on both the energy and angular distribution of beam electrons on the bremsstrahlung target as well as the type and thickness of materials that serve as filters between the bremsstrahlung and Compton targets. To relate the electron-beam voltage to the electron-to-x-ray dose ratio, photon spectra are calculated for monoenergetic electron beams incident on the bremsstrahlung target. The appropriate filters are applied to these spectra, which are convolved with the spectral responses of the *pin* diode and PCD detectors to

obtain the dose in each detector. The process is repeated for many values of the electron beam energy (E_{beam}) to obtain the dependence of the diode voltage on the dose ratio. In addition, it is well known that the bremsstrahlung radiation intensity is concentrated along the direction of the electron trajectory for $E_{\text{beam}} > 2$ MV.^{11,12} Therefore, sensitivity of the voltmeter to the electron angle of incidence on the bremsstrahlung target is expected. This issue is examined in detail below.

To proceed with the analysis, it is necessary to make some assumptions about the bremsstrahlung source. Therefore, the details that follow are for this particular source configuration. Fortunately, these calculations are relatively easy and different bremsstrahlung source configurations can be readily analyzed without having to repeat lengthy 3D calculations of the CH voltmeter. In the remainder of the article, the voltmeter is analyzed for the target/beam-stop/filter geometry used in the Gamble II experiments described in the next section. This geometry consisted of a planar, 0.01-cm-thick tantalum bremsstrahlung target followed by a 3-cm-thick aluminum beam stop. The source is further attenuated by a 0.6-cm-thick tungsten filter that is located at the entrance of the tungsten collimator. For the analysis presented here, the ITS codes are used to calculate photon spectra in this source configuration for electron beam energies ranging from 1 to 6 MeV in 1 MeV increments and incident electron angles on the bremsstrahlung target ranging from $\theta_{\text{inc}} = 0^\circ$ (normal incidence) to $\theta_{\text{inc}} = 80^\circ$ in 20° increments. Electrons backscattered into the diode are specularly reflected back into the target to mimic the effect of the large accelerating electric fields in the diode. The calculations for the radiation field are performed in 1D, converted into an equivalent point source, and then attenuated by $1/r^2$ to the position of the voltmeter located at 130 cm. The source spectra are calculated using 10 million primary electrons resulting in statistical uncertainties of 1%–2%. The spectra from these calculations are used in Eq. (2) to calculate both the Compton electron and x-ray doses from which the dependence of voltage on the electron-to-x-ray dose ratio (R) is formulated.

The dependence of the voltage on R and on electron angles of incidence with the voltmeter (VM) located in the forward direction ($\theta_{\text{VM}} = 0^\circ$, see Fig. 7) is shown in Fig. 3(a). At 1 MV, the voltage is insensitive to the angle of incidence. For voltages above 2 MV the voltmeter becomes increasingly sensitive to the electron incidence angle. For $R = 0.02$ the voltage is 2.0 ± 0.2 MV and for $R = 0.05$ the voltage is 4.0 ± 1.0 MV. Therefore, when the voltmeter is positioned in the forward direction, information about the electron angular distribution on the bremsstrahlung target is required to make accurate voltage measurements above 2 MV.

To understand the variation of R with the electron angle of incidence, it is important to note that the voltmeter response is sensitive to changes in the shape of the photon spectrum. The spectral shape depends not only on the end point (i.e., the voltage), but also depends on the relative angle between θ_{VM} and the incidence angle of the electron beam on the bremsstrahlung target (θ_{inc}), as well as the type and thicknesses of any filters. The calculated photon spectra

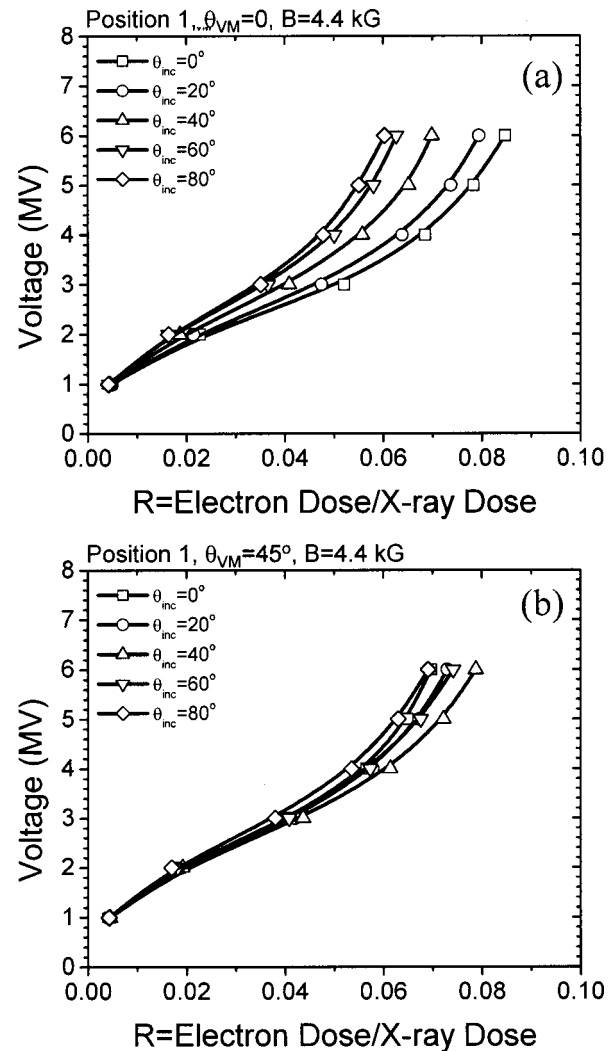


FIG. 3. Dependence of the voltage on the ratio of the electron dose to x-ray dose for different electron angles of incidence (θ_{inc}) on the bremsstrahlung target: (a) $\theta_{\text{VM}} = 0^\circ$ and (b) $\theta_{\text{VM}} = 45^\circ$.

in the forward direction ($\theta_{\text{VM}} = 0^\circ$) for $E_{\text{beam}} = 3$ MeV and different angles of incidence on the bremsstrahlung target are shown in Fig. 4(a). All the photon spectra have an end point that is consistent with the incident electron beam energy, but the forward-directed spectrum is considerably harder when the electron beam is normally incident ($\theta_{\text{inc}} = 0^\circ$). It is this variation in spectral shape that produces the variation in voltage with electron angle of incidence shown in Fig. 3(a).

The shape of the photon spectrum is also influenced by the materials that the photons must pass through to reach the Compton target. For the planar target geometry considered here, the thicknesses of these materials varies as $(\cos \theta_{\text{VM}})^{-1}$. Therefore, it is expected that the measured voltage also will be sensitive to the angular position of the voltmeter. The dependence of R on θ_{VM} for different angles of incidence and for $E_{\text{beam}} = 3$ MeV is shown in Fig. 5. The spread in R has a broad minimum for θ_{VM} from 45° to 65° . At $\theta_{\text{VM}} = 55^\circ$ the spread in R is reduced a factor of 4.5 compared to the spread in R at $\theta_{\text{VM}} = 0^\circ$. A similar reduction in the spread in R is also observed for $E_{\text{beam}} = 6$ MeV. In this case, the minimum spread in R occurs for $\theta_{\text{VM}} = 45^\circ$, and the

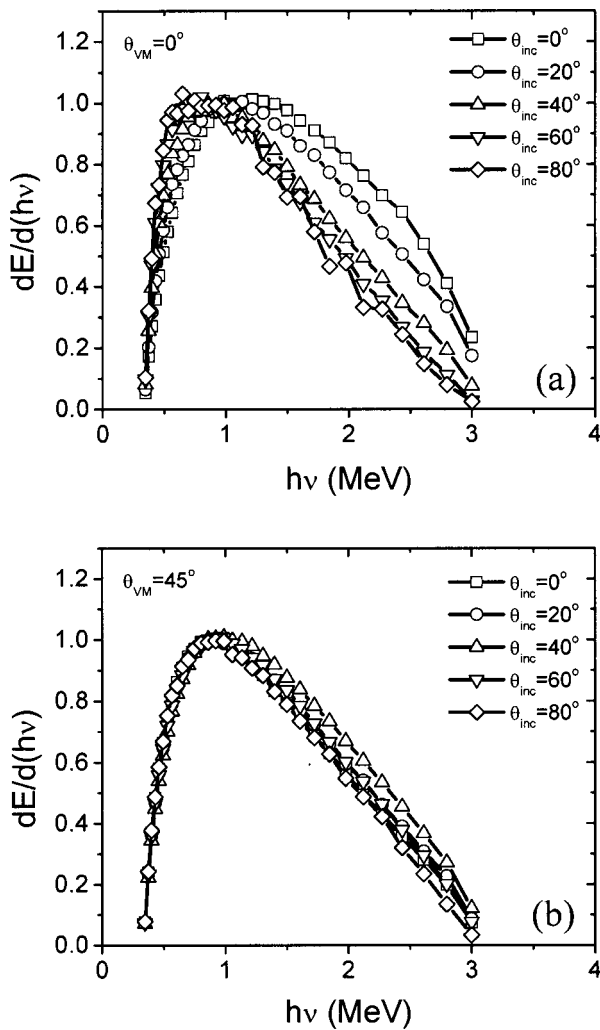


FIG. 4. Photon spectra calculated for different electron angles of incidence (θ_{inc}) on the bremsstrahlung target for $E_{beam} = 3.0$ MeV, and for (a) $\theta_{VM} = 0^\circ$ or (b) $\theta_{VM} = 45^\circ$.

spread in R is reduced a factor of 2.3 compared to the spread at $\theta_{VM} = 0^\circ$. For the bremsstrahlung target geometry analyzed here, $\theta_{VM} = 45^\circ$ provides a reasonable choice for minimizing the spread in R over the entire 2–6 MV voltage range.

The dependence of the voltage on R for $\theta_{VM} = 45^\circ$ is shown in Fig. 3(b). The large voltage spread for different angles of incidence at $\theta_{VM} = 0^\circ$ seen in Fig. 3(a) is greatly reduced when the voltmeter is positioned at $\theta_{VM} = 45^\circ$. At this location, the voltage is 2.0 ± 0.08 MV for $R = 0.02$ and 3.6 ± 0.3 MV for $R = 0.05$. The voltmeter is still somewhat sensitive to the electron angle of incidence at higher voltages. However, by proper choice of filters on the incident photon spectrum and location of the *pin* diode, it may be possible to further reduce the sensitivity of the voltage to electron angle of incidence for voltages above 4 MV.

The calculated photon spectra at $\theta_{VM} = 45^\circ$ for $E_{beam} = 3$ MeV is shown in Fig. 4(b). A comparison of Figs. 4(a) and 4(b) shows that the combined effects of the additional photon absorption by thicker materials along the line of sight between the source and the voltmeter and changes in the photon spectrum with incident electron angle cause less

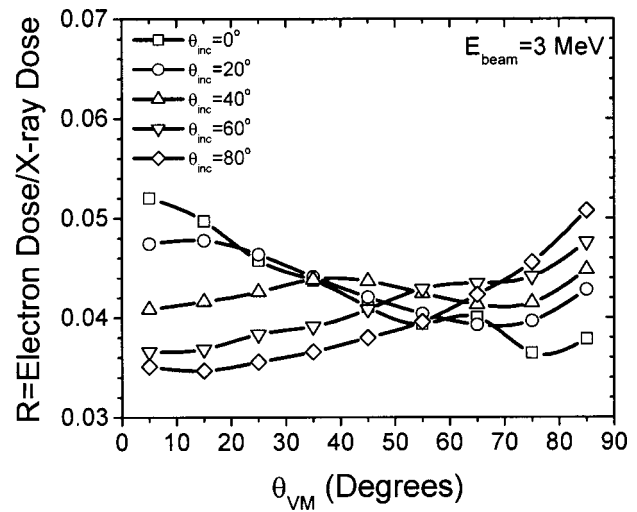


FIG. 5. Dependence of the electron-to-x-ray-dose ratio (R) on the voltmeter angle, θ_{VM} , for different electron angles of incidence (θ_{inc}) and $E_{beam} = 3.0$ MeV.

variation in the photon spectra with the electron angle of incidence when the voltmeter is positioned at $\theta_{VM} = 45^\circ$ than at $\theta_{VM} = 0^\circ$. It is this similarity of the spectral shapes that leads to a reduction in the sensitivity of the voltmeter to the angle of incidence.

The sensitive range of the voltmeter can be adjusted either by varying the applied magnetic field or the position of the *pin* diode relative to the Compton target. This sensitivity is shown in Fig. 6 for an isotropic angular distribution of electrons on the bremsstrahlung target with $\theta_{VM} = 0^\circ$. For voltages below 4 MV, the configuration with the *pin* diode in position 1 and $B = 4.4$ kG is superior to the other two configurations because the voltage is less sensitive to uncertainty in the measured dose ratio. For voltages above 4 MV, the configuration with the *pin* at position 1 and $B = 6.0$ kG gives a voltage that is slightly less sensitive to uncertainty in the measured dose ratio. The voltmeter is most sensitive to changes in the measured dose ratio for the configuration with

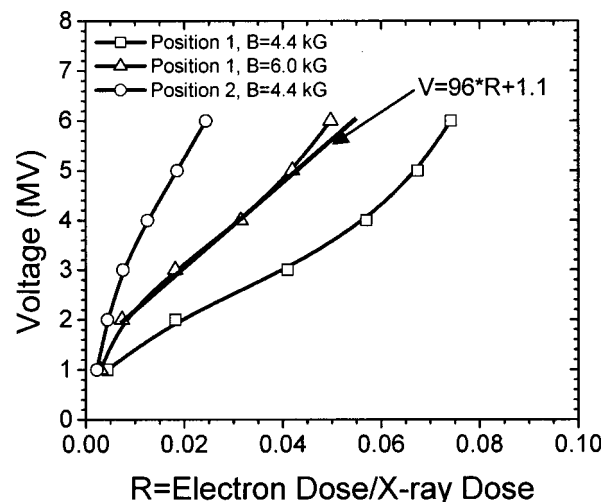


FIG. 6. Dependence of the voltage on the electron to x-ray dose for an isotropic electron beam with $\theta_{VM} = 0^\circ$ for $B = 4.4$ kG and $B = 6.0$ kG. The *pin* diode is located at 1.8 cm (position 1) or 2.8 cm (position 2) from the Compton target.

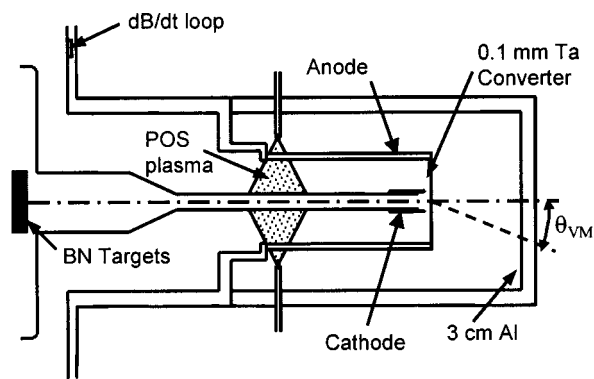


FIG. 7. Schematic of the POS and bremsstrahlung diode on Gamble II. The CH voltmeter is located 1 m from the Ta target at $\theta_{VM}=0^\circ$. BN targets are located inside the hollow cathode 70 cm from the from the Ta target.

the *pin* located in position 2 and $B=4.4$ kG. These sensitivities, along with the appropriate choice of filters, may be beneficial in developing a voltmeter to measure voltages outside the 2 to 5 MV range considered in this article.

III. EXPERIMENTS

The CH voltmeter is fielded on the Gamble II pulsed-power generator¹³ operated with a plasma opening switch (POS) to obtain voltages in the 2–5 MV range. The experimental geometry is shown in Fig. 7. Residual plasmas from the POS and the presence of vacuum electron flow between the switch and the bremsstrahlung diode load make determination of the voltage from electrical measurements difficult. A 0.1-mm-thick tantalum bremsstrahlung target is used with a 3-cm-thick aluminum beam stop. Due to experimental constraints, the CH voltmeter is fielded in the forward direction ($\theta_{VM}=0^\circ$) approximately 1 m from the bremsstrahlung source. In addition, a 6.0 kG magnetic field is used in the voltmeter since this choice is less prone to errors in the voltage due to errors in R at the upper end of the expected voltage range.

Since the voltmeter was fielded in the forward direction, Fig. 3 shows that the error associated with the electron angles of incidence is expected to be large. To reduce this error additional information is required about the electron angles on the bremsstrahlung target. To provide this information, the angular distribution of the radiation is measured by TLDs fielded at $\theta_{VM}=0^\circ$, 25° , $\pm 45^\circ$, and 65° . The TLDs consisted of a 1 mm \times 1 mm \times 6 mm parallelepiped of CaF₂ that, for equilibration purposes, was encased in a hollow, 6-mm-diam Al cylinder whose wall thickness was 2.3 mm. Each TLD is individually calibrated by exposing it to a known dose from a Co⁶⁰ source. Two TLDs are used at each location, averaged, and then compared with dose distributions calculated from the ITS code. The ITS calculations indicate the dose distribution from normally incident electrons is more forward directed than the measurements. Moreover, the measurements show that the measured radiation cannot be characterized by a single angle of incidence but that a distribution of angles is required. After several trials it was found that an isotropic electron distribution on the bremsstrahlung target reproduces the measured angular dose

distribution. In principle, there could be other distributions that also reproduce the TLD data. In addition, it is impossible to determine the time-varying angular distribution from the time-integrated TLD measurements. However, based on these data, an isotropic distribution of electrons on the bremsstrahlung target is a reasonable model for the electron angular distribution and is taken as an ansatz in the analysis of the Gamble II data. Therefore, the linear relationship shown in Fig. 6 is used to convert measured dose ratios into voltage in the Gamble II experiments. For critical applications of this technique, particle-in-cell simulations and/or time-resolved x-ray measurements of the angular distribution of the radiation could be used in conjunction with fielding the voltmeter at 45° to further reduce the uncertainty in the voltage due to the electron angular distribution.

An example of the application of the voltmeter to a Gamble II shot is shown in Fig. 8. The generator current, I_G , starts at $t=0$, and up to 340 kA flows through the POS plasma during the first 80 ns. Rapid opening of the POS produces a large voltage pulse as current is diverted from the POS and into the electron-beam diode. A combination of vacuum flowing electrons from the POS and electrons emitted from the diode strike the tantalum target and produce the bremsstrahlung radiation that is responsible for the signals measured in the voltmeter. An independent measurement of the radiation was obtained with a scintillator photodiode [dose rate in Fig. 8(a)].

The PCD and *pin* diode signals from which the dose ratio is calculated are shown in Fig. 8(b). The PCD and *pin* detectors are cross calibrated by exposing them simultaneously to 3–4 MV end-point bremsstrahlung from Gamble II, filtered by 2.5-cm-thick lead. The lead eliminates x rays below about 0.4 MeV. Transmitted x rays are absorbed in the detectors primarily by Compton processes, with approximately equal mass absorption coefficients for Si and GaAs. The dose in each detector is then equal to within about 10%. The dose ratio is converted into voltage (V_{CH}) using the linear relationship from Fig. 6, and is shown in Fig. 8(c). The peak voltage from the voltmeter is 3.7 ± 0.1 MV and is simultaneous with the peak in the x-ray signal. It is important to note that the quoted uncertainty is due to errors in the cross calibration of the detectors and does not include errors associated with the ansatz of an isotropic angular electron distribution on the bremsstrahlung target.

An independent measurement of the peak diode voltage is made with a nuclear activation diagnostic. Protons, accelerated across the diode, are directed onto boron nitride (BN) targets to produce ¹¹C radioactivity by the ¹¹B(*p*,*n*)¹¹C reaction. This reaction has a 3.0 MeV threshold and a cross section that exceeds 100 mb above 3.2 MeV.¹⁴ The thick-target yield for this reaction is given in Ref. 15. Positron decay of the ¹¹C radioactivity is measured after each shot by coincidence counting the 0.511 MeV γ rays with two NaI detectors.¹⁶ Corrections are made for the 20.4 min half life of ¹¹C to determine the initial activities. The decay of a BN target is followed for three half lives to confirm the 20.4 min decay of ¹¹C.

The BN targets are activated by protons extracted from impurities in the tantalum anode when the anode is heated by

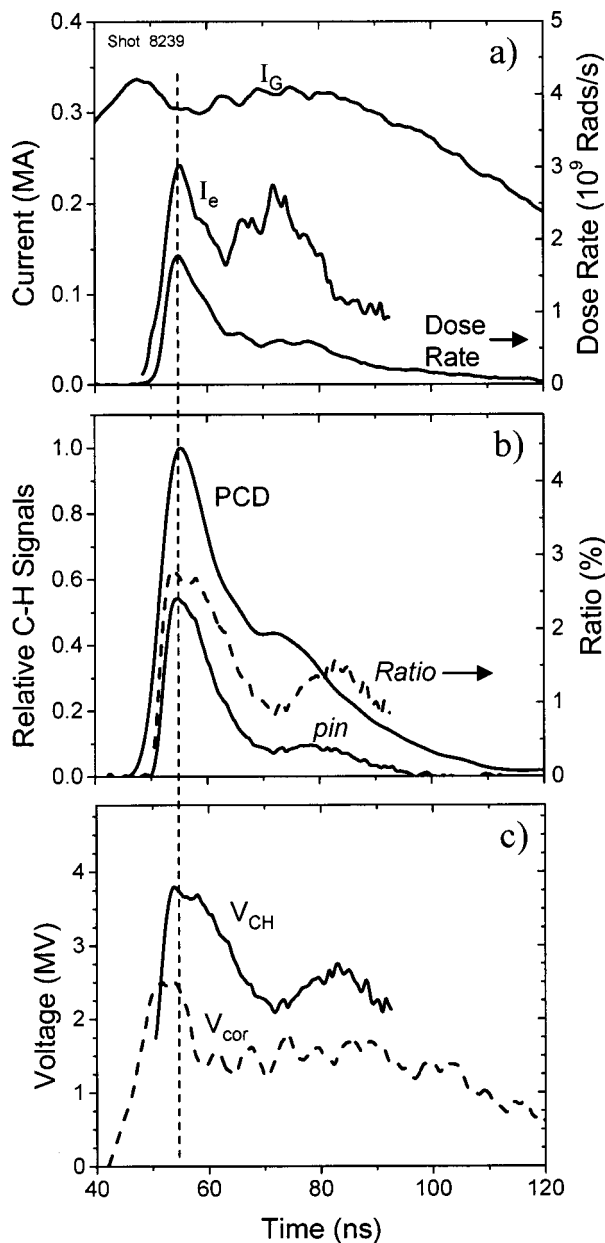


FIG. 8. (a) Total generator current (I_G), dose rate, and electron current (I_e) inferred from the dose rate using Eq. (3) for high-voltage POS shot 8239 on Gamble II. (b) Relative PCD and *pin* diode signals for this shot. The ratio of the PCD and *pin* diode signals is also shown. (c) Inductively corrected voltage (V_{cor}) and voltmeter voltage (V_{CH}) for this shot.

the intense electron pulse from the cathode. If the tantalum is degassed by heating the target to about 2000 K prior to the shot,¹⁷ impurities are driven out of the tantalum and the BN targets are not activated. This demonstrates that the protons originate from the tantalum anode. Protons, directed within the hollow cathode, are incident on the BN targets located 70 cm from the diode (see Fig. 7). A 5-cm-diam by 5-mm-thick BN disk is cut into quadrants to provide four equal-area targets. One of the quadrants of the BN disk is bare and the other three are covered with 18-, 36-, and 54- μm -thick aluminum foils. The thick-target yield is used to calculate the ratio of the activities induced in targets behind different thickness foils as a function of the incident proton energy. The measured ratio of activities is then used with the calcu-

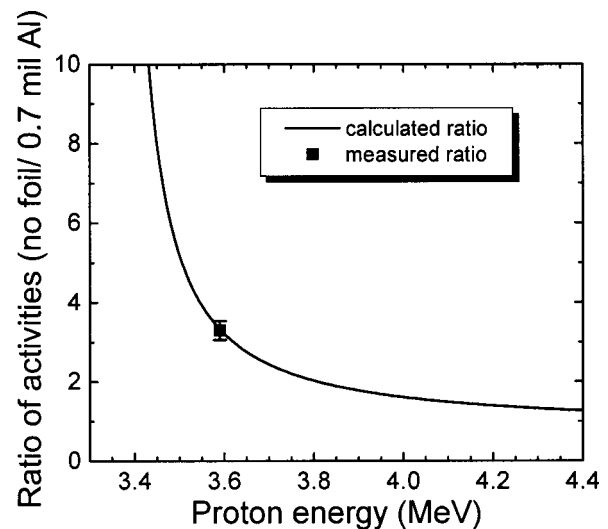


FIG. 9. Ratio of the ^{11}C activity for BN targets with no foil and with an 18-mm-thick Al foil as a function of incident proton energy. The curve is calculated from the thick-target yield. The square is the ratio measured on Gamble II shot 8239.

lated ratios to infer the proton energy, i.e., the diode voltage. No activity significantly above background is measured on the targets covered with 38- or 54- μm -thick foils. These foils are sufficiently thick to reduce the energy of most of the protons on the BN to less than the 3.0 MeV threshold energy. Activities significantly larger than background are measured on the targets covered with no foil or with a 18- μm -thick foil. The calculated ratio of activities and the measured ratio for these two targets are shown in Fig. 9. The calculated ratio is sensitive to protons of up to about 4 MeV. Thicker aluminum foils can be used for more energetic protons. The measured ratio in Fig. 9 is 3.30 ± 0.24 and the inferred proton energy is 3.59 ± 0.02 MeV, where the uncertainty is due to statistical counting. This voltage should be somewhat smaller than the peak diode voltage because this diagnostic measures the time-averaged voltage weighted by the thick-target yield. This voltage is consistent with the peak voltage of 3.7 MV from the CH voltmeter. Both the voltmeter voltage and the voltage from BN activation are much higher than the 2.5 MV peak from the inductively corrected voltage [V_{cor} in Fig. 8(c)].

Once the voltage is known, the electron current responsible for the measured dose rate can also be determined. To do this, the ITS simulations are used to obtain the relationship between the dose rate, voltage, and current. The result of these simulations for an isotropic electron distribution on the bremsstrahlung target and voltages between 1 and 5 MV is

$$\text{Dose rate} = 1.03 I_e V_{CH}^{1.46} [\text{kRad Si/s}], \quad (3)$$

where I_e is the electron current in A, and V_{CH} is the voltage in MV. The electron current obtained in this manner is shown in Fig. 8(a). The electron current at the time of peak dose rate is about 250 kA out of a total of approximately 300 kA. The inferred electron current is reasonable; for example, the remaining 50 kA could be ion current. The electron current inferred from the inductively corrected voltage produces a

peak electron current that is unphysically larger than the total current. Therefore, the corrected voltage (V_{cor}) is incorrect. This is likely the result of electrical failure of the dB/dt loop from which the inductive correction is obtained.

IV. DISCUSSION

The Compton–Hall voltmeter is a radiation-based voltage diagnostic developed to measure voltages on high-power (TW) pulsed generators. Photons from a bremsstrahlung diode are used to generate Compton electrons whose orbits are bent by an applied magnetic field and detected by a Si *pin* diode. The diode voltage is determined from the ratio of the electron dose to the x-ray dose. ITS simulations show that the voltmeter is sensitive to the shape of the photon spectrum. The shape of the photon spectrum is affected by the end point (i.e., the voltage) as well as by the electron angles of incidence on the target and by the thicknesses of any materials (filters) that the photons must pass through before reaching the detectors. For a planar target, differences in the spectral hardness of the photon spectra for electrons with different angles of incidence on the bremsstrahlung target are minimized at 45° with respect to the target. At this angle, the dependence of the measured voltage on the electron angles of incidence on the bremsstrahlung target is minimized and the instrument is relatively insensitive to the electron angle of incidence for voltages up to 4 MV. The uncertainty associated with unknown electron angles of incidence can be reduced further by incorporating the electron angular distribution on the bremsstrahlung target from either particle-in-cell simulations or direct measurements.

The curves relating voltage to dose ratio shown in Fig. 6 demonstrate the ability of this instrument to measure voltages not possible with filtered detectors (see Refs. 1 and 2). Although the relation between voltage and dose ratio has been developed only for voltages up to 6 MV, as long as there continues to be a one-to-one relationship between the voltage and R , it is relatively straightforward to extend these results to higher voltages. In addition, we have demonstrated that the sensitive voltage range can be adjusted by changing either the magnetic field or the position of the *pin* diode relative to the Compton target. Although not analyzed in the article, another possible way to affect the sensitive voltage range is to filter the *pin* diode and PCD separately to eliminate softer parts of the Compton electron and photon spectra. All of this flexibility makes it possible to design a voltmeter with a selectable range of operation.

The utility of the voltmeter was demonstrated on the Gamble II pulsed-power generator configured with a plasma opening switch to obtain voltages in the 2–4 MV range. Measurements on Gamble II produce a time-dependent voltage with a peak (3.7 MV) that agrees with nuclear activation measurements (3.59 MV) of boron–nitride targets and a

pulse shape that is consistent with the radiation pulse shape. Physically reasonable electron currents of 250 kA out of 300 kA total current are inferred from the measured dose rate and voltmeter voltage.

In the future, the CH voltmeter will be tested on Gamble II without a POS in the 1–2 MV range. In this range, the voltage electrically close to the load can be measured with a vacuum wire voltmeter¹⁸ and compared directly with the CH voltmeter. The uncertainty introduced by the cross calibration of the two detectors can be reduced by using detectors that are made of the same absorbing material. Therefore, the x-ray (PCD) detector may also be replaced with a Si *pin* detector. Application of the CH voltmeter to other diode configurations is being considered for rod-pinch diodes¹⁹ and other electron-beam diodes used for pulsed radiography²⁰ at voltages up to 14 MV.

ACKNOWLEDGMENTS

Rick Fisher, Eric Featherstone, David Phipps, and Aaron Miller are acknowledged for their technical expertise. This work was funded by The Defense Threat Reduction Agency.

- ¹J. C. Riordan, J. E. Faulkner, J. R. Goyer, D. Kortbawi, J. S. Meachum, R. S. Mendenhall, I. S. Roth, and B. A. Whitton, *Rev. Sci. Instrum.* **63**, 4792 (1992).
- ²S. G. Gorbics and N. R. Pereira, *Rev. Sci. Instrum.* **64**, 1835 (1993).
- ³J. A. Anderson *et al.*, *Nucl. Instrum. Methods Phys. Res. B* **40/41**, 1189 (1989).
- ⁴J. J. Carroll *et al.*, *Rev. Sci. Instrum.* **64**, 2298 (1993).
- ⁵S. A. Dan'ko, G. I. Dolgachev, Yu. G. Kalinin, and D. D. Maslennikov, *Plasma Phys. Rep.* **28**, 652 (2002).
- ⁶J. G. Kelly, L. D. Posey, and J. A. Hableib, *IEEE Trans. Nucl. Sci.* **NS-18**, 131 (1971).
- ⁷G. T. Baldwin and J. R. Lee, *IEEE Trans. Nucl. Sci.* **NS-33**, 1298 (1986).
- ⁸N. R. Pereira, S. G. Gorbics, and D. M. Weidenheimer, *Proceedings of the 11th International Conference on Particle Beams, Prague (1996)*, p. 1071.
- ⁹J. A. Halbleib, R. P. Kensek, G. D. Valdez, S. M. Seltzer, and M. J. Berger, *IEEE Trans. Nucl. Sci.* **41**, 1025 (1992).
- ¹⁰*Monte Carlo Transport of Electrons and Photons*, edited by T. M. Jenkins, W. R. Nelson, and A. Rindi (Plenum, New York, 1988).
- ¹¹W. W. Buechner, R. J. Van de Graaff, E. A. Burrill, and A. Sperduto, *Phys. Rev.* **74**, 1348 (1948).
- ¹²J. D. Jackson, *Classical Electrodynamics* (Wiley, New York, 1975), pp. 708–715.
- ¹³J. R. Boller, J. K. Burton, and J. D. Shipman, in *Proceedings of the 2nd IEEE International Pulsed Power Conference*, edited by A. H. Guenther and M. Kristiansen (1979), p. 205.
- ¹⁴G. F. J. Legge and I. F. Bubb, *Nucl. Phys.* **26**, 616 (1961).
- ¹⁵F. C. Young, S. J. Stephanakis, and D. Mosher, *J. Appl. Phys.* **48**, 3642 (1977).
- ¹⁶F. C. Young, J. Golden, and C. A. Kapetanacos, *Rev. Sci. Instrum.* **48**, 432 (1977).
- ¹⁷B. V. Weber, R. J. Allen, B. G. Moosman, S. J. Stephanakis, F. C. Young, N. R. Pereira, and J. R. Goyer, *IEEE Trans. Plasma Sci.* **30**, 1806 (2002).
- ¹⁸A wire voltmeter obtained from Titan Pulse Sciences Division (Part No. ZZM-16) can be used for voltages below 2 MV.
- ¹⁹G. Cooperstein *et al.*, *Phys. Plasmas* **8**, 4618 (2001).
- ²⁰J. E. Maenchen *et al.*, *Proceedings of the 14th International Conference on High-Power Particle Beams, Albuquerque, NM (2002)*, p. 117.